THE ASTROPHYSICAL JOURNAL, 372:L21–L24, 1991 May 1

THE H_2 LINE PROFILES IN THE CYGNUS LOOP: EVIDENCE FOR J-SHOCKS WITH MAGNETIC PRECURSORS

JAMES R. GRAHAM
Division of Physics, Math, and Astronomy, California Institute of Technology, 320-47, Pasadena, CA 91125
AND
GILLIAN S. WRIGHT AND T. R. GEBALLE
Joint Astronomy Center, 665 Komohana Street, Hilo, HI 96720
Received 1990 December 12; accepted 1991 February 11

ABSTRACT

We have obtained infrared Fabry-Perot spectra at ≈ 25 km s^{-1} resolution of the H_2 line emission associated with the fast shocks to the NE of the Cygnus Loop supernova remnant. Profiles of the 1–0 $S(1)$ H_2 emission associated with both the optically bright radiative shocks and the faint nonradiative shocks have been observed. The profiles are resolved and have deconvolved widths of ≈ 20 km s^{-1}. This result favors excitation of the H_2 emission in a magnetic precursor over excitation by a radiative precursor. Shocks with precursors may play an important role in Herbig-Haro objects, and in star-forming cloud cores.

Subject headings: infrared: spectra — interstellar: molecules — nebulae: individual (Cygnus Loop) — shock waves

1. INTRODUCTION

We have recently discovered 2 μm emission from vibrationally excited H_2 which is coincident with the optical shock-excited filaments to the northeast of the Cygnus Loop supernova remnant (Graham et al. 1991). Infrared imaging of the 1–0 $S(1)$ H_2 line shows a filamentary structure with a clear relationship to the optical line emission. One ridge of H_2 line emission lies 2′ beyond the edge of the remnant as delineated by the optically bright radiative shocks and is associated with the faint nonradiative shocks in this region. Other H_2 filaments are coincident with brighter radiative shocks. We deduced from optical shock diagnostics that the H_2 line emission in the Cygnus Loop comes from the regions where fast shocks (100 km s^{-1}) are propagating in low-density (5 cm^{-3}) gas. These are novel conditions for H_2 excitation. H_2 line ratios indicate a rotational-vibrational excitation temperature of 2200 ± 500 K. This low temperature rules out excitation mechanisms such as molecule formation and UV fluorescence. In Graham et al. (1991) we argue that the emission must be shock excited, not in the postshock flow where the conditions are too extreme for molecule survival, but rather in a magnetic shock precursor where temperatures are lower. Such a shock is intermediate between a simple hydrodynamic J-shock and a magnetohydrodynamic C-shock (Draine 1980). We have shown that excitation of H_2 in a magnetic precursor to a J-shock explains quantitatively the observed H_2 surface brightness, level population, and relation to optical emission.

Graham et al. (1991) considered a number of shock models with a range of shock velocities and preshock conditions which are appropriate for the Cygnus Loop and found that the peak temperature of the neutral gas in the precursor ranged from 16,000 to 60,000 K. In these models for the Cygnus Loop the gas density is well below the critical density for vibrational excitation of H_2, and consequently the excitation temperatures are much lower than the kinetic temperatures. The observed H_2 excitation temperature of 2200 ± 500 K favors models where the maximum precursor temperature is $\approx 20{,}000$ K, and therefore we expect the H_2 lines to have Doppler widths of ≈ 20 km s^{-1}. This Letter reports high spectral resolution observations of the H_2 1–0 $S(1)$ line from the Cygnus Loop and shows that the H_2 lines have widths of ≈ 20 km s^{-1}.

2. OBSERVATIONS

Infrared spectra of the 1–0 $S(1)$ line in the Cygnus Loop were obtained on nights of 1989 August and 1990 August at the UKIRT, Mauna Kea, Hawaii, under photometric conditions. The line profiles were measured using a scanning Fabry-Perot interferometer (FP) of nominal resolution 25 km s^{-1}, in series with the cooled grating spectrometer, CGS 2, which was set to a wavelength of 2.1218 μm to act as an order sorter. In 1989 the grating used had a 302 lines mm^{-1} grating providing a bandpass of 1200 km s^{-1}. In 1990 a 637 lines mm^{-1} grating was used which yielded a 450 km s^{-1} bandwidth. The free spectal range of the FP was 875 km s^{-1}, and therefore in both cases there was only one order transmitted to the detector. The beam of the instrument was approximately circular with a 4.″5 diameter. The wavelength calibration of the FP was determined by observations of lines from an argon discharge lamp, which were also used to determine the instrumental response. Lamp lines were observed at hourly intervals to monitor the instrumental profile and to measure the drift of the FP plate separation, which typically corresponded to 5 km s^{-1} per hour. Observations of the 1–0 $S(1)$ line were obtained by scanning the FP through 200 km s^{-1} in steps of 10 km s^{-1}. Each FP position was observed by integrating on the detector for 4×1.5 s. The sky was measured by nodding the telescope off source. A typical observation set consists of 10 object/sky pairs.

We observed three H_2 filaments identified as MH1, MH2, and MH4 in Figure 1 (Plate L1). Reduction of these observations consisted of shifting the wavelength of each scan according to the drift measured from lamp lines and then binning the data. Data from different nights were only added if the instrumental profile had not changed. In 1989 the FWHM of the lamp lines was measured to be 29–32 km s^{-1}, while in 1990 the FWHM was 26 km s^{-1}, so these data are presented separately. The argon lamp lines used to determine the spectral

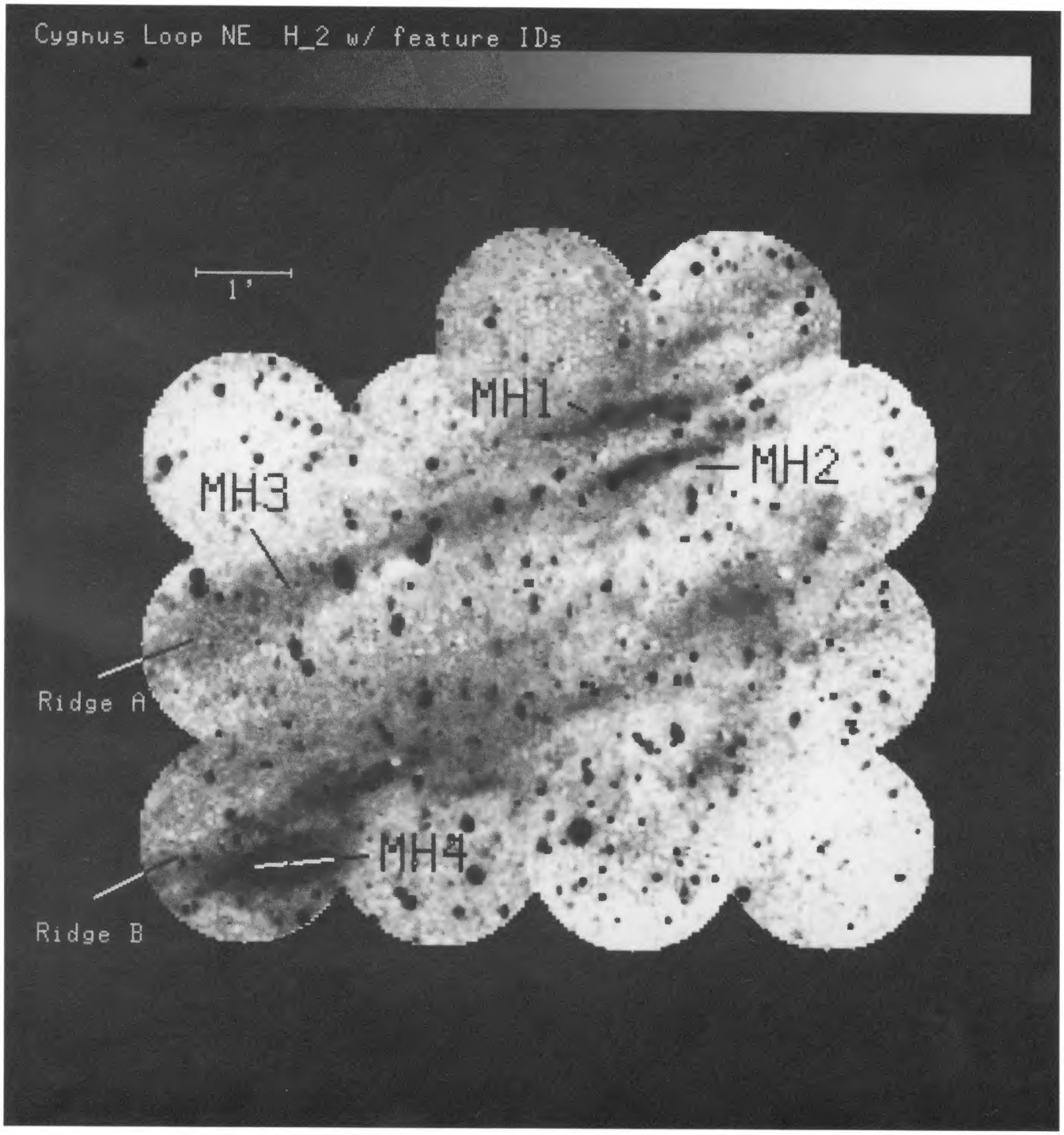

FIG. 1.—H_2 1–0 $S(1)$ mosaic of the NE part of the Cygnus Loop supernova remnant which shows the observed positions. Reproduced with permission from the Astronomical Journal (Graham et al. 1991). The image is not continuum subtracted, and many stars appear in the field. H_2 emission is associated with the bright optical emission in this region, but it is generally displaced in front of the edge of the optical line emission.

GRAHAM, WRIGHT, & GEBALLE (see 372, L21)

TABLE 1

H_2 1–0 $S(1)$ SPECTROSCOPY

Position	v_{LSR} (km s^{-1})	Observed FWHM[a] (km s^{-1})	FP FWHM[b] (km s^{-1})	Deconvolved FWHM[c] (km s^{-1})
MH1[d].....	4 ± 5	39 ± 5	26	21 ± 10
MH4[d].....	8 ± 4	50 ± 9	29	29 ± 16
MH1[e].....	4 ± 2	33 ± 2	23	19 ± 5
MH2[e].....	8 ± 2	34 ± 3	24	21 ± 6

[a] FWHM of best-fit Lorentzian.
[b] Instrumental FWHM corrected for the width of the Ar calibration line.
[c] FWHM of Gaussian component.
[d] 1989 data.
[e] 1990 data.

profile have pressure-broadened profiles with FWHM of ≈ 3 km s^{-1}. Therefore, the instrumental response used to deconvolve the H_2 line observations was taken to have the measured width minus 3 km s^{-1}. Table 1 lists the results: the 1–0 $S(1)$ FWHM, the v_{LSR} of the line center, and the deconvolved Gaussian FWHM of the line found by fitting a Voigt profile assuming a Lorentzian instrumental width (also tabulated) derived from observations of the argon lamp. Figure 2 shows the 1990 spectrum of MH1.

3. RESULTS

Table 1 shows that the observed H_2 line widths, determined from the best-fit Lorentzian, are all systematically broader than the instrumental resolution. The significance of the broadening ranges from the 90% to 99.99% confidence level, and therefore the evidence for having resolved the H_2 lines is convincing. If we assume that the H_2 lines are broadened by Poissonian effects, then the measured profile can be described by a Voigt function. We have determined the width of the Gaussian component by least-squares fitting the data by a Voigt function whose Lorentzian component width was determined from the argon lamp. This yields intrinsic line widths of 20–30 km s^{-1}. The reduced χ^2 for the fits to the model profiles is always less than 1. Therefore, the model is a good description of the data, and the error estimates are reliable. The measured line widths at the three different positions are all consistent within the errors. Therefore, it is reasonable to combine these observations. This yields a weighted mean FWHM of 20 ± 3 km s^{-1}, which, when interpreted as a thermal width, corresponds to a temperature of 17,000 ± 5000 K.

The velocities of the H_2 line centers lie in the range V_{LSR} = 4–8 km s^{-1}. Inspection of the position-velocity 21 cm H I maps of DeNoyer (1975) shows that the H I cloud in the vicinity of the NE filaments is found in the range V_{LSR} = 3–8 km s^{-1}. Thus, there is no evidence for acceleration of the excited H_2 along the line of sight.

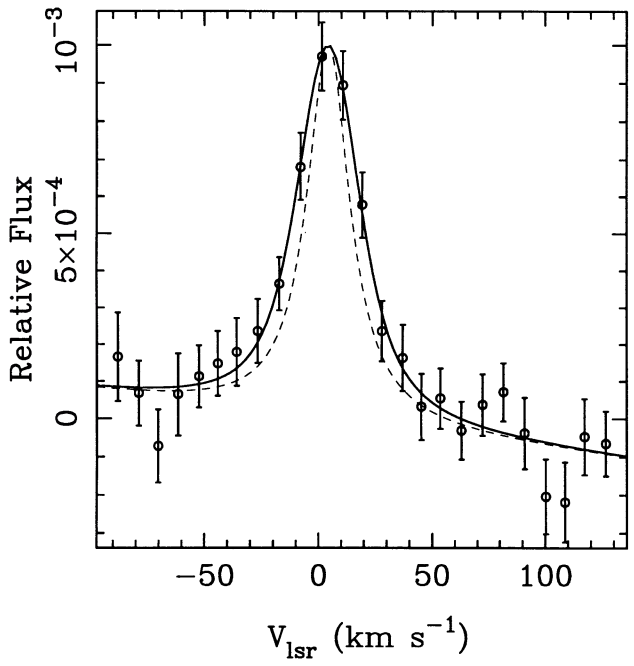

FIG. 2.—Fabry-Perot spectrum of the H_2 1–0 $S(1)$ line emission from MH1 in the Cygnus Loop. The observed FWHM of the line is 33 ± 2 km s^{-1}, while the resolution of the FP is 23 km s^{-1}, indicating that the line is resolved. Deconvolution of the line indicates an intrinsic Gaussian width of 19 ± 5 km s^{-1}. Dashed line is a normalized instrumental profile.

4. DISCUSSION

4.1. *The Cygnus Loop*

The detection of broad H_2 lines in the Cygnus Loop is important for understanding the nature of the emission because this result places new constraints on excitation mechanisms. We reconsider the excitation in the light of this data.

One important mechanism for exciting H_2 is UV pumping. The radiative shocks in this vicinity are a strong source of UV radiation, so a UV precursor may excite H_2 emission. Absoption of a UV photon by a H_2 molecule promotes it to an electronically excited state, and infrared line emission occurs as a consequence of the rotation-vibration cascade which ensues when the molecule decays back to an excited vibrational level of the ground electronic state. The fluorescent lines should be emitted at the ambient cloud velocity, and their widths should reflect the cloud's velocity dispersion (thermal and turbulent). The preshock gas to the NE of the Cygnus Loop is a diffuse H I cloud, and therefore fluorescent line widths should be no more than a few km s^{-1}. High-resolution spectroscopy of the UV-excited sources, NGC 2023, Parsamyan 18, and the Orion Bar, show that the H_2 lines are considerably narrower than Burton et al.'s (1990) instrumental resolution of 16 km s^{-1}. Consequently, the considerably greater widths of the H_2 lines in the Cygnus Loop tend to rule out UV fluorescence and reinforce the arguments against it based on the rotation-vibration level population and energetics, presented in Graham et al. (1991).

Another form of radiative precursor which should be considered is X-ray heating. Lepp & McCray (1983) have shown that a molecular cloud heated by a compact X-ray source will convert approximately 10% of the absorbed X-ray luminosity into H_2 line emission. In their model the H_2 line emission is excited in gas with $T < 4000$ K, and thus the thermal line width from an X-ray–heated gas cloud is $\lesssim 10$ km s^{-1}, well below that observed in the Cygnus Loop. However, the physical conditions considered by Lepp & McCray are quite different from those in the Cygnus Loop; their models have much higher density and X-ray flux. Therefore, we have estimated the effects of X-ray heating in the Cygnus Loop. The X-ray flux incident on the H_2 filaments is found by assuming the highest X-ray surface brightness of 6.6×10^{-5} ergs s^{-1} cm^{-2} sr^{-1} measured by Ku et al. (1984). The temperature of the emitting gas is $\approx 3 \times 10^6$ K, so the typical photon energy is 0.3 keV (Ku et al.). The gas will be heated by photoionization, for which the

cross section is $9.3 \times 10^{-21}(E/0.3\ \mathrm{keV})^{-3}\ \mathrm{cm}^{-2}$, appropriate for cosmic abundances and assuming H is in molecular form (Brown & Gould 1970). Balancing this heating rate with the H_2 rotational-vibrational cooling function of Hollenbach & McKee (1979) yields equilibrium temperatures of 1400–400 K ($\Delta v = 6$–$3\ \mathrm{km\ s^{-1}}$) for $n_{H_2} = 1$–$10\ \mathrm{cm^{-3}}$. It is clear that the temperature in X-ray–heated gas close to the Cygnus Loop will be too low to account for the observed broad lines. This calculation also gives the H_2 1–0 $S(1)$ volume emissivity of X-ray–heated gas and can be used to show that the surface brightness of an H_2 filament with $n_{H_2} = 1\ \mathrm{cm^{-3}}$ is $I = 4.7 d_{16} \times 10^{-12}$ ergs $\mathrm{s^{-1}\ cm^{-2}\ sr^{-1}}$, where d_{16} is the depth of the filament along the line of sight in units of 10^{16} cm. If a typical filament depth is similar to the projected length of the H_2 filaments (1′–5′), then we expect $I = 3$–15×10^{-10} ergs $\mathrm{s^{-1}\ cm^{-2}\ sr^{-1}}$. This brightness is many orders of magnitude fainter than the observed range of $I = 4$–20×10^{-6} ergs $\mathrm{s^{-1}\ cm^{-2}\ sr^{-1}}$. We therefore conclude that X-ray heating is not a viable alternative.

The most natural explanation for supersonic H_2 line widths is surely one which invokes shocks. Shocks can easily account for large velocity dispersions due to strong heating and acceleration. There is a strong observational selection effect for shock fronts which are close to tangency to the line of sight, because of the resultant geometric enhancement of the surface brightness. Current infrared techniques restrict high-resolution spectroscopy to the brightest features in the Cygnus Loop, and therefore it is not surprising that no large velocity shifts of the line center have been found there. In Graham et al. (1991) we explored several shock models, for example, slow shocks in a population of dense molecular cloudlets, but the only satisfactory solution was excitation in the magnetic precursor to a fast shock. The precursor model predicts that the molecular material entering the shock be heated to $\gtrsim 10^4$ K. For example, the model with $v_s = 87\ \mathrm{km\ s^{-1}}$, $n_{H_2} = 2\ \mathrm{cm^{-3}}$, and $B = 8\ \mu$G has a maximum precursor temperature of 16,500 K. The H_2 level population measured in Graham et al. (1991) favors models with a peak precursor temperature of $\approx$20,000 K. Therefore, failure to detect H_2 line widths of at least 20 km $\mathrm{s^{-1}}$ would constitute a clear failure of the precursor model. Broad H_2 lines are detected with widths close to that expected, and therefore the precursor model passes this test.

Although our results are consistent with the precursor model, we cannot rule out that another type of shock may account for our observations. The current data cannot distinguish between intrinsically broad lines and lines broadened by a macroscopic velocity dispersion, for example, caused by ripples in the shock front. Thus, observations with higher angular resolution than the present ones are an important further test of the precursor model.

There is some indirect evidence, from optical observations, that the H_2 line width is due to thermal broadening. The width of the narrow component of the Hα line from nonradiative shocks measures the temperature of the gas before it enters the shock. Hester & Raymond (1988, 1990) have found from high-resolution spectroscopy of the nonradiative shocks in the Cygnus Loop that the narrow component has a width of $\approx$25 $\mathrm{km\ s^{-1}}$, which is much broader (i.e., hotter) than expected for the cool preshock medium. If precursor heating accounts for the width of the narrow component of Hα from nonradiative shocks and the H_2 excitation, then the H_2 line width should be $\approx 25/\sqrt{2}\ \mathrm{km\ s^{-1}} = 18\ \mathrm{km\ s^{-1}}$, which is consistent with the measured H_2 width. This coincidence suggests that the same process—a shock precursor—is responsible for the broad Hα and H_2 lines.

4.2. *Shock Precursors in Other Regions*

The formation of a precursor can occur under a variety of interstellar conditions, and therefore other shock-excited H_2 sources may involve shocks with precursors. A shock will have a magnetic precursor when the shock speed is less than the ion magnetosonic speed (Draine 1980). This condition may be expressed as $B_{-6}^2 > 8.3 n_H v_7^2 (x/3 \times 10^{-4})$, where B_{-6} is the magnetic field in μG, n_H is the H number density, v_7 is the shock velocity in 100 $\mathrm{km\ s^{-1}}$, and x is the fractional ionization; 3×10^{-4} is appropriate for a diffuse cloud (see Graham et al. 1991). If the magnetic field is given by $B_{-6} = b n_H^{1/2}$, then the condition becomes $v_7 < 0.35 b (x/3 \times 10^{-4})^{-1/2}$. For the Cygnus Loop $b \approx 5$ (Raymond et al. 1988), so there will be a precursor if $v < 175\ \mathrm{km\ s^{-1}}$. For dense molecular gas $x \approx 10^{-7}$ and $b \approx 1$ (Hollenbach & McKee 1989), and the critical velocity is $v < 2000\ \mathrm{km\ s^{-1}}$. Consequently the shocks in dense molecular gas such as in Herbig-Haro objects and star-forming cloud cores are good candidates for shocks with precursors.

We must remember that when conditions of steady flow are established behind a fast shock, UV emission from the postshock recombination zone will photoionize preshock gas, increasing x to unity. Thus to be self-consistent an additional requirement for the formation of a precursor is that either (1) the age of the shock is less than the postshock cooling time, for example, the shock is a nonradiative Balmer shock or an "incomplete" shock, or (2) the shock is too slow to cause substantial preionization. Condition 1 holds for the shocks in the Cygnus Loop with H_2 emission.

J-shocks with precursors have been invoked by Hartigan, Curiel, & Raymond (1989) to explain the correlation between Hα, [S II] and H_2 emission in HH 7–11. There is evidence that magnetic shock precursors are present in other HH objects. The strong correlation between optical and H_2 emission observed in HH 43 has been explained by a J-shock which reforms H_2 downstream of the shock (Schwartz et al. 1988). However, precursor excitation will account for this morphology without invoking molecule reformation. Cohen et al. (1988) have proposed a model to explain the infrared line emission from HH objects, including HH 7–11 and HH 43, in which fast J-shocks account for the [O I] 63 μm emission, while slower C-shocks in denser gas are responsible for the H_2 emission. A shock with a magnetic precursor might explain these data without invoking two density components and therefore may be a simpler solution. HH 7–11 and HH 43 are low-excitation HH objects (Hartigan, Raymond, & Hartman 1987). Their spectra are dominated by strong [S II] and [O I], and there is no [O III], which indicates $20 < v_s/\mathrm{km\ s^{-1}} < 30$ (Hartigan et al. 1987). The preionization in such a shock will be negligible (Shull & McKee 1979), and the conditions for a precursor will be met.

The Orion BN/KL region, which has been studied in greater detail than other regions of H_2 line emission, is an example of a molecular outflow encountering an ambient molecular cloud. Two shocks develop as a result of this interaction. An outer shock is driven into the molecular cloud, while an inner shock develops in the wind. H_2 line emission appears to be detected from the wind and the cloud (Geballe et al. 1986; Geballe & Garden 1990). Detailed modeling (e.g., Chernoff, Hollenbach, & McKee 1982; Draine & Roberge 1982; McKee & Hollen-

bach 1987; Hollenbach & McKee 1989) has suggested that C-shocks ($v_s \approx 40$ km s^{-1}) in the ambient cloud can account for the H_2, CO, and OH emission, while a dissociative wind J-shock ($v_s \approx 70$ km s^{-1}) is responsible for the fine-structure and radio recombination line emission. This model provides an incomplete account of the H_2 observations because the slow C-shocks cannot explain the presence of high-velocity (100 km s^{-1}) H_2 line wings (Geballe et al. 1986); the model has been called into question on other observational grounds as well (Brand et al. 1988). If the H_2 data is interpreted in terms of simple shocks, then the highest velocities cannot reflect the shock speed in stationary gas because such fast shocks would dissociate H_2. A solution is to invoke a third system of slow nondissociative shocks in the fast molecular protostellar wind (Chevalier 1980; Nadeau, Geballe, & Neugebauer 1982; Geballe et al. 1986). The origin of the third system of slow wind shocks is obscure. A physically motivated explanation for the high-velocity H_2 emission is that it is excited in a magnetic precursor to the wind J-shock. Since the H_2 emission is excited in the molecular outflow from IRc 2, rather than the ambient material, the line widths will reflect the wind velocity. If the wind shock is part of a steady flow, with a complete cooling and recombination zone, the upstream gas will be ionized and the precursor destroyed. Therefore, the IRc 2 wind shock must be incomplete, like the fast shocks in the Cygnus Loop with H_2 emission, so that it has suppressed UV emission. This may be accomplished if the wind is either intermittent or inhomogeneous.

5. CONCLUSIONS

High-resolution spectroscopy of the H_2 filaments in the Cygnus Loop verifies the prediction of the J-shock precursor model for the H_2 filaments in the Cygnus Loop that the 1–0 $S(1)$ line has a width of ≈ 20 km s^{-1}. This result is inconsistent with UV pumping or X-ray heating models. A J-shock precursor accounts for all of the infrared observations and explains anomalous aspects of the Hα emission from the nonradiative shocks to the NE of the Cygnus Loop. Observations of shock-excited H_2 in HH objects and star-forming cloud cores may also be explained by shock precursors. Therefore, J-shocks with magnetic precursors may be common and constitute an important class of astrophysical shock waves which warrant detailed study.

We wish to acknowledge the excellent support at the UKIRT provided by T. Wold, D. M. Walther, and all of the observatory staff who made these observations possible. UKIRT is operated by the Royal Observatory Edinburgh on behalf of the UK Science and Engineering Research Council. JRG is supported in part by National Science Foundation grant AST 86-13059.

REFERENCES

Brand, P. W. J. L., Moorhouse, A., Burton, M. G., Geballe, T. R., Bird, M. C., & Wade, R. 1988, ApJ, 334, L103
Brown, R. L., & Gould, R. J. 1970, Phys. Rev. D., 1, 2252
Burton, M. G., Geballe, T. R., Brand, P. W. J. L., & Moorhouse, A. 1990, ApJ, 352, 625
Chernoff, D. F., Hollenbach, D. J., & McKee, C. F. 1982, ApJ, 259, L97
Chevalier, R. A. 1980, Ap. Letters, 21, 57
Cohen, M., Hollenbach, D. J., Haas, M. R., & Erikson, E. F. 1988, ApJ, 329, 863
DeNoyer, L. K. 1975, ApJ, 196, 479
Draine, B. T. 1980, ApJ, 241, 1021
Draine, B. T., & Roberge, W. G. 1982, ApJ, 259, L91
Geballe, T. R., & Garden, R. P. 1990, ApJ, 383, 602
Geballe, T. R., Persson, S. E., Simon, T., Lonsdale, C. J., & McGregor, P. J. 1986, ApJ, 302, 693
Graham, J. R., Wright, G. S., Hester, J. J., & Longmore, A. J. 1991, AJ, in press
Hartigan, P., Curiel, S., & Raymond, J. 1989, ApJ, 347, L31
Hartigan, P., Raymond, J., & Hartmann, L. 1987, ApJ, 316, 323
Hester, J. J., & Raymond, J. C. 1988, Supernova Remnants and the Interstellar Medium, ed. R. S. Roger & T. L. Landecker (Cambridge: Cambridge University Press), 415
———. 1991, in preparation
Hollenbach, D. J., & McKee, C. F. 1979, ApJS, 41, 555
———. 1989, ApJ, 342, 306
Ku, W. H.-M., Kahn, S. M., Pisarski, R., & Long, K. S. 1984, ApJ, 278, 615
Lepp, S., & McCray, R. 1983, ApJ, 269, 560
McKee, C. F., & Hollenbach, D. J. 1987, ApJ, 322, 275
Nadeau, D., Geballe, T. R., & Neugebauer, G. 1982, ApJ, 253, 154
Raymond, J. C., Hester, J. J., Cox, D., Blair, W. P., Fesen, R. A., & Gull, T. R. 1988, ApJ, 324, 869
Schwartz, R. D., Williams, P. M., Cohen, M., & Jennings, D. G. 1988, ApJ, 334, L99
Shull, J. M., & McKee, C. F. 1979, ApJ, 227, 131